Mol Cell Neurosci. Author manuscript; available in PMC 2015 November 01.

Published in final edited form as:
Mol Cell Neurosci. 2014 November ; 63: 83–95. doi:10.1016/j.mcn.2014.10.006.

Vascular pathology of 20-month-old hypercholesterolemia mice in comparison to triple-transgenic and APPSwDI Alzheimer's disease mouse models

Lindsay A. Hohsfield[a], **Nina Daschil**[a], **Greger Orädd**[b], **Ingrid Strömberg**[b], and **Christian Humpel**[a,*]

[a]Laboratory of Psychiatry and Experimental Alzheimer's Research, Department of Psychiatry and Psychotherapy, Medical University of Innsbruck, A-6020 Innsbruck, Austria

[b]Department of Integrative Medical Biology, Umeå University, SE-901 87 Umeå, Sweden

Abstract

Several studies have shown that elevated plasma cholesterol levels (i.e. hypercholesterolemia) serve as a risk factor for late-onset Alzheimer's disease (AD). However, it remains unclear how hypercholesterolemia may contribute to the onset and progression of AD pathology. In order to determine the role of hypercholesterolemia at various stages of AD, we evaluated the effects of high cholesterol diet (5% cholesterol) in wild-type (WT; C57BL6) and triple-transgenic AD (3xTg-AD; Psen1, APPSwe, tauB301L) mice at 7, 14, and 20 months. The transgenic APP-Swedish/Dutch/Iowa AD mouse model (APPSwDI) was used as a control since these animals are more pathologically-accelerated and are known to exhibit extensive plaque deposition and cerebral amyloid angiopathy. Here, we describe the effects of high cholesterol diet on: (1) cognitive function and stress, (2) AD-associated pathologies, (3) neuroinflammation, (4) blood–brain barrier disruption and ventricle size, and (5) vascular dysfunction. Our data show that high dietary cholesterol increases weight, slightly impairs cognitive function, promotes glial cell activation and complement-related pathways, enhances the infiltration of blood-derived proteins and alters vascular integrity, however, it does not induce AD-related pathologies. While normal-fed 3xTg-AD mice display a typical AD-like pathology in addition to severe cognitive impairment and neuroinflammation at 20 months of age, vascular alterations are less pronounced. No microbleedings were seen by MRI, however, the ventricle size was enlarged. Triple-transgenic AD mice, on the other hand, fed a high cholesterol diet do not survive past 14 months of age. Our data indicates that cholesterol does not markedly potentiate AD-related pathology, nor does it cause significant impairments in cognition. However, it appears that high cholesterol diet markedly increases stress-related plasma corticosterone levels as well as some vessel pathologies. Together, our findings represent the first demonstration of prolonged high cholesterol diet and the examination of its effects at various stages of cerebrovascular- and AD-related disease.

*Corresponding author at: Department of Psychiatry and Psychotherapy, Anichstrasse 35, A-6020 Innsbruck, Austria. christian.humpel@i-med.ac.at (C. Humpel).

Europe PMC Funders Author Manuscripts

Keywords

Alzheimer's disease; Hypercholesterolemia; Cholesterol; β-Amyloid; Tau; Neuroinflammation; Vascular pathology; Learning; Memory; MRI

1. Introduction

Alzheimer's disease (AD) is a progressive neurodegenerative disease characterized by the deposition of β-amyloid (Aβ)-associated senile plaques and tau-associated neurofibrillary tangles (Querfurth and LaFerla, 2010). Although convincing evidence indicates that Aβ plays a causal role in early-onset AD pathology, finding the disease-causing factor in late-onset AD has proved difficult due to the multi-faceted and complex nature of this disease (Bertram et al., 2010; Hardy and Selkoe, 2002).

Impaired cholesterol metabolism is one of many mechanisms implicated in the etiology and progression of late-onset AD (Gamba et al., 2012; Maulik et al., 2013; Puglielli et al., 2003). Several epidemiological investigations have shown that elevated plasma cholesterol (hypercholesterolemia) is an established risk factor for late-onset AD and that lowering cholesterol levels through the use of statins can reduce this risk (Gamba et al., 2012; Haag et al., 2009; Reiss and Voloshyna, 2012). However, clinical trials using statins have produced mixed and conflicting results (Di Paolo and Kim, 2011). In addition to hypercholesterolemia, one of the major risk factors for late-onset AD is the inheritance of the ApoE ε4 allele, a protein responsible for cholesterol transport in the brain (Beel et al., 2010; Bu, 2009). Several genome-wide association studies have also demonstrated that mutations in genes associated with cholesterol metabolism result in increased susceptibility to late-onset AD (Jones et al., 2010; Lambert et al., 2013).

Furthermore, animal studies have shown that hypercholesterolemia can induce cognitive deficits and AD-like neuropathology including Aβ plaque deposition and tau hyperphosphorylation (Ghribi et al., 2006; Granholm et al., 2008; Schreurs, 2010; Sparks et al., 2000; Thirumangalakudi et al., 2008). Our lab and others have shown that non-transgenic animals fed a high cholesterol diet exhibit enhanced Aβ deposition, blood–brain barrier (BBB) breakdown, and inflammatory marker expression (Ghribi et al., 2006; Schreurs et al., 2012; Sparks et al., 2000; Ullrich et al., 2010). Previous studies have also demonstrated that hypercholesterolemia accelerates Aβ load (Refolo et al., 2000) and interneuronal Aβ oligomer accumulation (Umeda et al., 2012) in AD transgenic mice, however, these studies have focused on relative acute effects of cholesterol diet (7–8 weeks).

Taken together, these investigations suggest that hypercholesterolemia may play a role in AD etiology. However, the exact mechanism of how cholesterol affects AD pathology and cognitive impairment remains unclear (Wood et al., 2014). Recent studies indicate that enhanced cholesterol can promote the proteolytic processing of amyloid-precursor protein (APP) as well as the subsequent aggregation and fibrillization of Aβ (Beel et al., 2010; Gamba et al., 2012; Maulik et al., 2013). Although it is not fully understood how elevated blood cholesterol levels correlate to brain cholesterol levels, it is hypothesized that vascular dysfunction and the loss of BBB integrity due to Aβ accumulation enhance the influx of

cholesterol or cholesterol metabolites into the brain (Shobab et al., 2005). It seems possible that hypercholesterolemia could promote increased cerebrovascular and BBB damage, ultimately leading to the influx of neurotoxic molecules and enhanced inflammatory processes, followed by alterations in AD pathology and the initiation of neurodegeneration and cognitive deficits (Sagare et al., 2013).

The aim of the present study was to better understand the relationship between hypercholesterolemia and AD-related pathology. Specifically, we were interested in the effects of high cholesterol diet on AD-related neuropathology, cognitive function, neuroinflammation, and cerebrovascular changes in wild-type and transgenic AD mice at various ages and stages of disease. We hypothesize that elevated cholesterol induces vascular dysfunction, aggravates Aβ and tau pathology and cognitive impairment as well as promotes neuroinflammation. Here, we chose to evaluate the effects of prolonged cholesterol diet (5–18 months) and systematically characterize the effects of this chronic diet treatment on vascular impairment, cognitive function and AD-like pathology. The present study provides evidence that high cholesterol diet can alter cognitive function, aggravate Aβ interneuronal cortical staining, promote glial cell activation and complement-related pathways, enhance the infiltration of blood-derived proteins and alter vascular integrity.

2. Results

2.1. Body weight gain and plasma cholesterol levels

WT mice significantly gained weight at 7 ($p > 0.001$) and 20 ($p > 0.001$) months, whereas 3xTg-AD mouse weights remained relatively unchanged (Table 2). At 14 months, however, 3xTg-AD cholesterol-fed mice significantly lost weight ($p > 0.05$) compared to 3xTg-AD mice on normal diet. Unfortunately, all 3xTg-AD cholesterol-fed mice did not survive to 20 months.

Cholesterol plasma levels were measured following fourteen weeks on cholesterol diet. High cholesterol diet in WT mice induced a significant ($p < 0.01$) increase in plasma cholesterol levels (1.28 ± 0.12 mg/ml) compared to WT mice on normal diet (0.71 ± 0.07 mg/ml). Interestingly, 3xTg-AD mice (1.12 ± 0.15 mg/ml) also display significantly ($p < 0.05$) higher cholesterol levels compared to WT mice. Although cholesterol-fed 3xTg-AD mice do not seem to gain significant weight, they show a significant increase ($p < 0.05$) in cholesterol levels compared to 3xTg-AD mice fed normal diet.

2.2. Cognitive functions assessed in the 8-arm radial maze

To determine whether cholesterol diet has an effect on cognitive function, animals were evaluated for spatial learning and memory performance in our previously described 8-arm radial maze using the win-shift procedure (Ullrich et al., 2010). At 7 months, spatial memory, measured as entries to repeat during retention, was significantly reduced in both WT cholesterol-fed ($p < 0.01$) and 3xTg-AD normalfed ($p < 0.001$) animals compared to WT normal-fed control mice (Fig. 1A). Interestingly, 3xTg-AD cholesterol-fed mice exhibited memory retention similar to WT cholesterol-fed animals and did not appear to present significantly more aggravated cognitive deficits compared to 3xTg-AD normal-fed

animals (Fig. 1A). At 14 months, only 3xTg-AD mice exhibited a significant ($p < 0.01$) decline during spatial learning testing (Fig. 1D). Again, cholesterol-fed 3xTg-AD mice appeared slightly improved compared to 3xTg-AD on normal diet (Fig. 1D). However, it should be noted that working memory errors and total arm visits were significantly reduced in both 3xTg-AD normal- ($p < 0.01$) and cholesterol-fed ($p < 0.05$) animals during these learning sessions (Fig. 1E & F). At 20 months, 3xTg-AD normal-fed mice exhibited significantly ($p < 0.05$) decreased entries to repeat during learning trials (Fig. 1D). However, again both 3xTg-AD and WT cholesterol-fed animal groups exhibited significantly reduced working memory errors and total arm visits during retention (spatial memory testing) (Fig. 1B & C), indicating that some impairments are present in these animals. Unfortunately, all 3xTg-AD cholesterol-fed mice did not survive to 20 months.

2.3. Plasma corticosterone levels

At 14 months, WT cholesterol-fed mice exhibited significantly ($p < 0.05$) reduced plasma corticosterone, a biomarker for stress (Goymann et al., 2002), levels compared to WT normal-fed mice. 3xTg-AD mice on cholesterol diet, on the other hand, exhibited significantly enhanced levels compared to both WT cholesterolfed ($p < 0.001$) and transgenic mice ($p < 0.05$) on normal diet (Table 3).

2.4. Cortical Aβ and tau pathology

At 7, 14, and 20 months no positive Aβ immunostaining was apparent in either WT (Fig. 2A) or WT cholesterol-fed (Fig. 2B) animals. At 7, 14, and 20 months 3xTg-AD mice exhibited Aβ (4–5 kD)-positive interneuronal cortical immunostaining, however, there were no visible signs of Aβ-positive plaques (Fig. 2C & I). We also tested staining for other Aβ peptide isoforms, including $Aβ_{1–16}$ and $Aβ_{13–28}$, however, again we observed no plaque deposition in the cortex or any other brain regions (not shown). As a positive control, APPSwDI mice were evaluated at 12 months for cortical Aβ. These animals displayed extensive plaque deposition (Fig. 2D & J) as well as Aβ-positive vessels and neurons in the cortex (not shown). Although cholesterol diet did not induce Aβ-positive staining in WT mice, 3xTg-AD cholesterol-fed mice exhibited significantly enhanced cortical Aβ interneuronal staining at 7 months ($p < 0.05$) and slightly elevated staining at 14 months compared to 3xTg-AD mice fed on normal diet (Fig. 2I).

Cortical staining for hyper-phosphorylated tau (phosphor-paired helical filament (PHF)-tau), observed in the form of both neurons and tangles, was also enhanced in 3xTg-AD cholesterol-fed mice compared to normal-fed mice, however, not significantly (Fig. 2K). Unlike Aβ staining, which was strictly localized to the cortex, tau-positive staining was observed in the cortex, hippocampus, subiculum, and amygdala regions (not shown).

2.5. Inflammatory markers

Neuroinflammation was assessed using the following immune-related markers: GFAP, a marker for reactive astrocytes, Iba1, a macrophage/microglia-specific marker which is upregulated during cell activation, and C1q, which recognizes one of the first subcomponents of the serum complement system. At 7 and 14 months, cholesterol-fed WT mice showed little to no differences in GFAP and Iba1 staining patterns in the cortex

compared to normal-fed WT mice (Fig. 3M & N). However, at 20 months GFAP (Fig. 3A, B & M) and Iba1 (Fig. 3E, F & N) cortical immunostaining patterns were significantly enhanced ($p < 0.01$ and $p < 0.001$, respectively) in WT animals receiving cholesterol diet compared to animals on normal diet. In 3xTg-AD and at all time-points GFAP staining was significantly ($p < 0.05$ or $p < 0.001$) elevated (Fig. 3C & M).

Iba1 staining was only significantly ($p < 0.001$) elevated in 3xTg-AD mice at 20 months, displaying strong single cell staining patterns (Fig. 3G & N). Cholesterol-fed 3xTg-AD mice showed no elevation in immune cell staining patterns and in most cases this staining appeared even slightly reduced in comparison to normal-fed animals (Fig. 3M & N). APPSwDI mice were again used as a positive control and exhibited the most pronounced GFAP and Iba1 cortical staining (Fig. 3D, H, M & N).

At 7 and 14 months, cholesterol-fed 3xTg-AD mice displayed the highest C1q staining patterns seen within all groups, apart from APPSwDI positive controls (Fig. 3O). Furthermore, at 7 months cholesterol-fed 3xTg-AD mice displayed a significantly ($p > 0.05$) elevated number of C1q-positive lesions compared to normal-fed 3xTg-AD mice (Fig. 3O). In WT animals, cholesterol diet slightly enhanced C1q staining at 7 and 20 months, however not significantly (Fig. 3I, J, & O). At 20 months, C1q was pronounced throughout the cortex, hippocampus, and other brain regions in 3xTg-AD mice similar to positive control APPSwDI mice (Fig. 3K, L, & O).

2.6. Blood–brain barrier disruption

Serum protein infiltration of IgG and ApoE was used to assess disruptions in BBB integrity. Between 7 and 14 months, IgG-positive lesions were only visible in positive control APPSwDI mice (Fig. 4D & I). At 20 months, some IgG lesions were visible in WT (Fig. 4A), WT cholesterol-fed (Fig. 4B), and 3xTg-AD (Fig. 4C) mice with transgenic mice displaying the most deposition (Fig. 4C). However, no significant difference in cortical IgG leakage was found between animal groups (Fig. 4I). Interestingly, it appeared that most IgG-positive staining began in or progressed from the hippocampus. Here, we observed more IgG-positive neurons in the hippocampus of WT cholesterol-fed (Fig. 4B, inset; Fig. 4J) mice compared to WT normal-fed (Fig. 4A, inset) mice, as well as, enhanced deposition of IgG-positive lesions, neurons, and vessels in the hippocampus of APPSwDI mice at 12 months (Fig. 4D, inset; Fig. 4J).

ApoE is also a plasma protein as well as cholesterol/lipid transporter that is thought to play a role in vessel disorders (Grinberg and Thal, 2010). We found no apparent or visible difference in cortical ApoE immunostaining between animal groups (Fig. 4E–H) at any time point. However, at 20 months we observed enhanced ApoE neuronal staining in the hippocampus of WT cholesterol-fed (Fig. 4F, inset) and 3xTg-AD normal-fed (Fig. 4G, inset) animals compared to WT normal-fed animals (Fig. 4E, inset; Fig. 4K). APPSwDI mice displayed enhanced ApoE staining at 12 months (Fig. 4H, inset; Fig. 4K). The ApoE staining pattern was also different in these mice compared to 3xTg-AD mice, where APPSwDI mice exhibited more lesion- or vessel-like ApoE staining rather than neuronal staining seen in WT cholesterol-fed and 3xTg-AD mice.

2.7. MRI analysis

The FLASH sequence was chosen to study the events of micro-bleedings in the brain, however, no microbleedings were found. Instead, a change in the size of the lateral ventricles was detected. A significant difference in the ventricle size between genotypes was found at the level of bregma ($F_{4, 61} = 3.267$, $p < 0.05$, two-way ANOVA), while no interaction between genotypes and time was observed ($p > 0.05$). Further caudally in the brain, the lateral ventricles appeared much enlarged, lateral to the hippocampus (Fig. 5). These enlarged ventricles were found in 3xTg-AD mice at 14 and 20 months and in 3xTg-AD mice treated with cholesterol diet at 7 months. This observation was neither found in WT nor in APPSwDI mice at any time point. In fact, the lateral ventricles of APPSwDI measured at bregma level were significantly smaller than those in cholesterol-fed WT animals and those in 3xTg-AD mice, treated with and without cholesterol-enriched diet.

2.8. Vessel pathologies

Blood vessel morphology and vascular pathology were assessed using collagen IV and transglutaminase 2. Collagen IV serves as a major component of basement membranes, including the cerebrovascular basement membrane, and is used to detect extracellular matrix proteins (Bourasset et al., 2009). At 7 and 14 months, we observed no significant differences in blood vessel structure or formation, as seen by positive collagen staining, between WT, WT cholesterol-fed, 3xTg-AD, and 3xTg-AD cholesterol-fed animals (not shown). At 20 months, WT cholesterol-fed mice displayed significantly ($p < 0.01$) darker blood vessel staining (Fig. 6B), measured as optical density, as well as, significantly ($p < 0.01$) fewer vessel branches, and slightly longer branch lengths (Fig. 6I) compared to WT normal-fed mice (Fig. 6A). 3xTg-AD mice showed no significant difference in collagen IV optical density, however, exhibited significantly ($p < 0.05$) fewer branches (Fig. 6C & I) compared to WT normal-fed animals. At 12 months, APPSwDI mice displayed low collagen IV optical density staining (Fig. 6I). Interestingly, APPSwDI mice exhibited an increased number of vessel branches unlike 3xTg-AD mice (Fig. 6D & I).

Tissue transglutaminase 2 is an enzyme involved in protein cross-linking. It can bind to the extracellular matrix and is thought to play a role in apoptosis, CAA pathology, and extracellular matrix development (Filiano et al., 2010; Wilhelmus et al., 2012). Here, we observed two different staining patterns for transglutaminase 2 in the cortex: vessel-like and lesion-like pathologies (Fig. 6E–H). At 7 months, transglutaminase-positive vessels were present in the cortex, however, did not vary in number or morphology between animal groups (Fig. 6J). At this same time point, little to no transglutaminase-positive lesion staining was observed (Fig. 6K). At 14 months, lesions were present in the cortex and significantly ($p < 0.01$) elevated in 3xTg-AD cholesterol-fed mice (Fig. 6K). Vessel staining was also elevated at 14 months and significantly ($p < 0.05$) enhanced in WT cholesterol-fed mice (Fig. 6J). At 20 months, contrary to 14 month observations, lesions were only visible in WT mice (Fig. 6E). Vessel staining was, however, significantly ($p < 0.05$) enhanced in WT cholesterol-fed mice (Fig. 6F & J).

Europe PMC Funders Author Manuscripts

3. Discussion

In the present study, we investigated the effects of hypercholesterolemia on WT and transgenic AD mice including: (1) cognitive function and stress, (2) AD-like pathologies, (3) neuroinflammation, (4) BBB disruption and (5) vascular dysfunction (Table 4). We hypothesized that cholesterol diet would exert disease-modifying effects on these cortical properties dependent on the age and stage of cerebrovascular- or Alzheimer-related disease.

Table 4. This table provides an overview of the various outcomes and pathologies that were observed in the four investigated mouse models over the course of this study. WT and 3xTg-AD mice were fed either a normal or 5% cholesterol (CHOL) diet from age 2 months and onwards. Animal weight and plasma cholesterol levels were measured to examine the effects of diet. Cognitive function, measured as entries to repeat during learning and retention (memory) session, was evaluated in an 8-arm radial maze. Corticosterone was used as a marker for stress. Regions of the cortex and hippocampus were examined for signs of AD-like pathology (i.e. β-amyloid (Aβ) and phospho-paired helical filament (PHF)-tau), neuroinflammation (i.e. glial fibrillary acid protein (GFAP), ionized calcium binding adapter molecule 1 (Iba1), and C1q), blood–brain barrier (BBB) disruption (i.e. anti-mouse Immunoglobulin G (IgG) and apolipoprotein E (ApoE)), and vessel staining or abnormalities (collagen IV and tissue transglutaminase 2 (tTG-2)). The table above provides an overview of the various outcomes and pathologies that were observed in the four investigated mouse models during this study. NA: not applicable, arrows indicate significant increase/decrease, arrows in parenthesis indicate slight trend, =: unchanged. All mouse models compared to WT on normal diet, except for 3xTg-AD + CHOL animals which were compared against 3xTg-AD animals.

3.1. Hypercholesterolemia as a model for AD

Several in vitro and in vivo studies have demonstrated that cholesterol modification (via dietary consumption or in culture) induces Aβ production and promotes the formation of Aβ plaques and tau hyperphosphorylation (Di Paolo and Kim, 2011; Gamba et al., 2012; Ghribi, 2008). In rabbits, it has been shown that hypercholesterolemia (by 2% cholesterol diet for 8 weeks ± copper in drinking water) induces learning and memory impairment (Darwish et al., 2010; Schreurs et al., 2013), AD-like pathology (i.e. interneuronal and extracellular Aβ accumulation and tau hyperphosphorylation), vascular inflammation (Sparks et al., 2000), astrocytosis, microglial activation (Xue et al., 2007), and reduced acetylcholine (Perez-Garmendia et al., 2014). Our lab has previously reported that rats fed a 5% cholesterol diet for 5 months exhibit impaired learning and long-term memory, cholinergic dysfunction, enhanced Aβ and tau levels, inflammation, and enhanced BBB leakage (Ullrich et al., 2010).

In the present study, WT mice were fed the same 5% cholesterol diet and exhibited a significant increase in weight gain and plasma cholesterol levels as expected. However, in our hands this cholesterol diet in mice was not as effective at inducing AD-like pathologies or cognitive deficits as our previously described rat model, which after 5 months of diet exhibits severe cognitive impairment. Although we observed an increase in immune cell activation and alterations in blood vessel pathologies at 20 months, only a weak decline in cognition was observed in the WT cholesterol-fed mice. Interestingly, these animals exhibit

more pronounced memory impairments at 7 months. These findings suggest that over prolonged cholesterol diet, the brain or processes involved in promoting memory-related neuroplasticity may be able to compensate for initial cognitive deficits brought on by hypercholesterolemia.

Others have reported that C57BL/6 mice fed a high fat/cholesterol diet for 8 weeks exhibit impaired working memory and activated hippocampal microglia and astrocytes (Thirumangalakudi et al., 2008). We also observed that elevated cholesterol diet results in enhanced hippocampal ApoE immunoreactivity in WT animals. As previously mentioned ApoE plays an important role in cholesterol metabolism and transport, and it has been suggested that changes in cholesterol metabolism can alter its expression in the periphery and brain (Petanceska et al., 2003). In support of our findings, several studies have demonstrated that high cholesterol diet results in increased brain ApoE levels, indicating that modifying peripheral cholesterol levels can lead to changes in ApoE expression. One study demonstrated that loading cholesterol in primary glial cells causes increased production of cellular and secreted ApoE (Petanceska et al., 2003), suggesting that glial cells may play a role in cholesterol-mediated ApoE brain levels.

3.2. Transgenic mouse models of AD

The APPSwDI (Tg-SwDI) transgenic mouse model was first established and described by Davis et al. (2004). These mice exhibit severe Aβ-associated pathology, in the form of interneuronal and plaque-like staining, which begins around 3–6 months. These animals also demonstrate severe vascular Aβ deposition, or cerebral amyloid angiopathy (CAA), which is mainly restricted to the thalamus area. In the present study we used this model as a positive control since these animals show markedly enhanced Aβ plaques, neuroinflammation and BBB disruptions. We were interested in determining whether cholesterol diet could aggravate AD pathologies via vascular disruption in 3xTg-AD mice. Since APPSwDI mice exhibit extensive CAA pathology at 12 months these animals were chosen as a positive control. Vascular abnormalities, in the form of collagen IV- and transglutaminase 2-positive vessel staining, were not as apparent in the cortex of these animals. However, we demonstrate, to our knowledge, for the first time that C1q and ApoE staining is significantly altered in APPSwDI mice.

Several investigations have previously described and characterized the 3xTg-AD mouse model in detail (Billings et al., 2005; Hunter et al., 2011; Oddo et al., 2003; Sterniczuk et al., 2010). Earlier studies reported that this model exhibits apparent extracellular Aβ deposition by 6 months of age, however, we and others (Hirata-Fukae et al., 2008; Hunter et al., 2011) have found this pathology to be markedly delayed (i.e. 14–18 months). In this study, we observed interneuronal Aβ immunostaining in the cortex as early as 6 months, however, we observed no apparent deposition of extracellular Aβ plaques by 20 months. It could be possible that these delayed pathologies may be a result of genetic shifting or the lack of recognition of a particular plaque-forming Aβ isoform by our investigated Aβ antibodies. Similar to previous studies which have reported that PHF-1 pathology does not become evident until 18 months (Hunter et al., 2011; Oddo et al., 2003), we also did not observe pronounced PHF-tau pathology until animals reached 20 months of age. At this time,

animals exhibited tau-positive pyramidal neuron and dystrophic neurite staining, however, no visible signs of neurofibrillary tangle deposition.

Our data also show that cognitive function is markedly impaired in 3xTg-AD mice without any significant changes in body weight or plasma stress-related corticosterone levels, which might be explained by the enlarged lateral ventricles found at the hippocampal level. We do, however, observe a significant increase in plasma cholesterol levels in these animals. By 20 months, neuroinflammatory processes are extensive, however, less pronounced than those observed in our positive control APPSwDI mice. At this stage, IgG infiltration is slightly more evident in 3xTg-AD animals, however, again less extensive than in APPSwDI control mice. In addition, vessel abnormalities are nearly absent in the animals with the exception of reduced vessel branches. Here, it is interesting to note that in both transgenic AD models, neuroinflammation appeared to be the most pronounced neuropathology, with the exception of Aβ and tau pathology.

3.3. Effects of cholesterol diet on AD-like and neuroinflammatory pathologies in triple-transgenic AD mice

Previous investigations have indicated that hypercholesterolemia can potentiate AD-like pathology in 3xTg-AD mice (Refolo et al., 2000; Umeda et al., 2012). However, in the present study, our data show that prolonged 5% cholesterol diet does not markedly increase Aβ and tau staining in 3xTg-AD mice and does not result in significant cognitive impairment at 7 or 14 months. Unfortunately, 3xTg-AD mice in this study did not survive to 20 months with cholesterol diet. Since the 3xTg-AD cholesterol-fed mice exhibited accelerated mortality and these animals visited significantly fewer arms during cognitive testing, it would be interesting to characterize more early behavioral impairments. Future studies should involve testing these animals for changes in sensory and behavioral/motor competence as well as other cognitive measures (e.g. Morris water maze and object recognition).

One of the most striking results from our study was the lack of significant weight gain by 3xTg-AD mice following cholesterol diet, despite the fact that plasma cholesterol levels are enhanced after 14 weeks of diet. To our knowledge, we are the first to report these findings. A recent study by Knight et al. report that non-Tg and 3xTg-AD mice gain comparable body weight when fed a high-fat diet, in which animals receive 13% saturated fatty acids (Knight et al., 2014). Although this data differs from our findings, it could indicate that hypercholesterolemia plays a different role on fat distribution compared to high fat intake or obesity. Furthermore, this data suggests that AD-associated genotypes (i.e. the presence of AD-related transgenes) may be involved in cholesterol metabolism in the periphery and its subsequent accumulation in fatty tissues. This may also explain why normal diet-fed 3xTg-AD mice also display heightened plasma cholesterol levels. Hyperactivity has previously been described in 3xTg-AD animals and it has been reported that APP mice exhibit more anxiety-like behavior at 9 months compared to WT mice (Bedrosian et al., 2011). In support of our findings, an earlier study has shown that ApoE knockout mice exhibit increased plasma corticosterone levels as well as increased anxiety behavior in the elevated plus maze (Raber, 2007). Together, these findings suggest that AD-related genes and cholesterol

modification may play a role in elevated stress and anxiety, which may contribute to body weight changes.

Our data shows that cholesterol diet given for 5 months (i.e. 7-month-old animals) in 3xTg-AD aggravates interneuronal Aβ cortical accumulation and C1q cortical deposition. In an earlier study, it was reported that hypercholesterolemia accelerates Aβ accumulation and AD-related pathology in APP transgenic mice (Refolo et al., 2000). More recently, it has been demonstrated that hypercholesterolemic APP transgenic mice, but not control APP transgenic mice or hypercholesterolemic non-transgenic littermates, exhibit memory impairment, interneuronal accumulation of Aβ oligomers, synaptic loss, and abnormal tau phosphorylation in the hippocampus (Umeda et al., 2012). These findings suggest that in mice high cholesterol diet can only aggravate existing AD pathology rather than induce this pathology in non-transgenic mice. It could be possible that other factors may be needed to induce AD pathology in non-transgenic mice (i.e. presence of copper or iron). To our knowledge, this is the first study to show that cholesterol diet in AD transgenic diet aggravates C1q deposition. Similar to our findings, Knight et al. (2014) report that high-fat diet results in negative effects on memory through changes associated with neuroinflammation (e.g. microglial activation), independent of alterations in Aβ or tau neuropathology.

3.4. Vascular pathologies in hypercholesterolemia and AD

According to several studies, vascular risk factors, such as hypercholesterolemia, hyperhomocysteinemia and hypotension, may play an important role in the development and cognitive decline of AD (de la Torre, 2013; Humpel, 2011; Iadecola, 2013; Sagare et al., 2013; Zlokovic, 2008). Here, we report that in both WT and 3xTg-AD mice hypercholesterolemia results in the significant reduction of collagen-positive blood vessel branches and an elevation in transglutaminase 2-positive staining, but significant only in WT cholesterol-fed animals. In WT mice, cholesterol diet leads to elevated immunoreactivity of transglutaminase 2 in blood vessels. In 3xTg-AD mice, cholesterol diet leads to enhanced deposition of transglutaminase 2-positive lesions in the cortex. In agreement with our data, previous investigations have described the following alterations in vascular pathology of AD transgenic mice: microvascular degeneration and abnormalities (including decreased vascular densities, BBB impairment, as seen by increased presence of Ig and albumin, in the vicinity of amyloid plaques (Kumar-Singh et al., 2005)), reduction in cerebrovascular volume, increase in basement membrane thickening (Bourasset et al., 2009), age-related microvascular pathology, reduced microvascular length, abnormal immunostaining of basement membrane-associated antigens, and thickening of the vascular basal laminae (Gama Sosa et al., 2010). A recent study by Grammas and colleagues has also shown that 3xTg-AD mice exhibit vascular activation and inhibiting this activation can improve cognitive function (Grammas et al., 2014). Recent investigations in non-transgenic animals have shown that rabbits fed 2% cholesterol diet for 10–12 weeks exhibit increased ventricular volume and narrowed cerebrovascular diameter (Deci et al., 2012; Schreurs et al., 2013).

Although the exact role of transglutaminase 2 in AD pathology is not fully understood, some suggest that it may be responsible for modulating processes involved in cell survival after insult and serve as a marker for CAA (Filiano et al., 2010; Wilhelmus et al., 2012). It could be possible that cholesterol diet and mechanisms involved in AD-associated transgene expression promote ischemia, BBB alterations or CAA-like pathology resulting in vascular disruption. However, further studies are needed to fully characterize the mechanisms involved in these dysfunctions. Taken together, these findings indicate that cholesterol diet and AD-associated transgenes can alter vascular pathology and possibly play a role in potentiating cerebrovascular- and AD-related pathological progression.

3.5. Ventricle alterations in hypercholesterolemia and AD

Ventricular enlargement is one of the most common anatomical hallmarks of AD (Deci et al., 2012; Nestor et al., 2008). In addition, a recent study by De Reuck and colleagues has reported a high incidence of white matter changes (62%) as well as several vascular-related abnormalities: lacunes (16%), macro-infarcts (31%), micro-infarcts (16%), macro-bleeds (24%), micro-bleeds (18%), mini-bleeds (89%) and CAA (58%) present in the human postmortem AD brain (De Reuck et al., 2011).

In the present study we used MRI analysis to measure the incidence of micro-bleeds, white matter and ventricle size changes in response to cholesterol diet. Micro-bleeds usually appear as round approx. 2-10 mm diameter black radiological spots on MRI images. Here, we could not detect micro-bleeds in any of our animal groups at any time point, suggesting that these are either not present or that these vessel lesions are too small to detect compared to more visible human brain lesions. The Swedish, Dutch, and Iowa APP mutations are all associated with CAA and higher incidence of hemorrhagic strokes and/or infarcts (Philipson et al., 2010). Thus, we were surprised that no micro-bleeds were detected in APPSwDI mice, our positive control mice. On the other hand, we observed a significant enlargement in ventricles in cholesterol-fed wildtype mice and normal-fed 3xTg-AD mice compared to wildtype mice on normal diet at 14 months. Similar to these findings, Deci and colleagues report that 2% cholesterol diet significantly increases ventricular volume in New Zealand White rabbits (Deci et al., 2012). Further in line with our data, Xie and colleagues found that rTg4510 transgenic AD mice exhibit increased dilation of the lateral ventricles compared to wildtype mice (Xie et al., 2010). Others have also reported that intracisternal injection of Aβ results in increased thickness of the lateral ventricles in aged rats (Ramesh et al., 2011).

To our knowledge, we are the first to report on ventricle size changes in wildtype and 3xTg-AD mice with and without cholesterol treatment as well as in APPSwDI mice. We were surprised to find that the lateral ventricles were reduced in cholesterol-fed 3xTg-AD mice and APPSwDI mice. Others have reported that following the introduction of a strong presenilin mutation, Aβ generation shifts towards the 42 isoform, effectively elevating parenchymal Aβ levels and reducing vascular amyloid deposition (Beckmann et al., 2011; Herzig et al., 2004). It could be possible that the presence of certain Aβ isoforms and/or elevated vascular amyloid deposition could play a role in ventricle size alterations. We were also surprised to find that, contrary to another report suggesting ventricular enlargement is a function of age, all animal groups, except 3xTg-AD cholesterol-fed mice, exhibited either

similar or reduced ventricular size changes over time (Chen et al., 2011). Together, our data indicates that AD-related transgenes as well as cholesterol diet can alter lateral ventricular volumes.

4. Conclusions

The present study provides evidence that high cholesterol diet can differentially alter weight, cognitive function, AD-related pathology, neuroinflammation, and vascular pathologies in WT and 3xTg-AD mice depending on age and stage of disease. To our knowledge, this is the first study that examines the effects of prolonged cholesterol diet in both WT and 3xTg-AD at various stages of disease. These findings suggest that neuroinflammation and cerebrovascular dysfunction including ventricle enlargement, in addition to abnormal Aβ and tau accumulation, may also play a role in disease onset and progression, providing important implications for the development of new therapeutic approaches against late-onset AD.

5. Experimental methods

5.1. Animals and diet

Wildtype (WT, 129/C57BL6), triple-transgenic Alzheimer's disease (3xTg-AD, B6; 129-*Psen1*^{tm1Mpm}Tg(APPSwe, tauB301L)1Lfa/J) and transgenic APPSwDI (Tg-SwDI; expressing amyloid precursor protein (APP) harboring the Swedish K670N/M671L, Dutch E693Q, and Iowa D694N mutations; C57BL/6-Tg(Thy1-APPSwDutIowa) BWevn/Mmjax) mice were purchased from The Jackson Laboratory and housed at the Innsbruck Medical University animal facility providing open access to food and water under 12 h/12 h light–dark cycles. All experiments were performed with male mice to avoid any effects from gender differences.

All animals were genotyped according to standardized methods. Briefly, DNA was extracted from a 0.5 cm-long mouse tail snip using Qiagen's DNeasy Kit (Hilden, Germany) following the manufacturer's instructions. Microsynth generated the required primers to detect APP gene expression: forward primer: 5′-AGG ACT GAC CAC TCG ACC AG-3′ and reverse primer: 5′-CGG GGG TGT AGT TCT GCA T-3′. Primers were amplified via polymerase chain reaction (PCR) with thermocycling conditions set as follows: initial denaturation at 94 °C for 3 min (1 cycle), denaturation at 94 °C for 30 s (35 cycles), annealing at 52 °C for 1 min (35 cycles), extension at 72 °C for 1 min (35 cycles), and final extension at 72 °C for 2 min (1 cycle). Amplified DNA was stored at 4 °C. To detect DNA bands gel electrophoresis was performed on a 3% agarose gel and DNA was visualized by GelRed™ Nucleic Acid Gel Stain (Biotium, Hayward, USA). APP-positive DNA bands were detected under UV light at 377 bp.

At 2 months of age, animals began to receive either a normal diet or a well-established 5% cholesterol diet (Ullrich et al., 2010) and continued the diet regimen until reaching 7, 14, or 20 months of age. The diet consisted of: 450 g/kg cornstarch, 140 g/kg casein, 155 g/kg maltodextrin, 100 g/kg sucrose, 40 g/kg soybean oil, 50 g/kg fiber, 35 g/kg mineral mix, 1.8 g/kg L-Cystine, 1.4 g/kg choline chloride, 0.0008 g/kg butylhydroxytoluol, 10 g/kg vitamin

mix (without folic acid), 1 g/kg chocolate aroma, and 0.002 g/kg folic acid with an additional 50 g/kg cholesterol for animals on the cholesterol diet (Ssniff special diet GmbH; Soest Germany). All animal experiments were approved by the Austrian Ministry of Science and Research (BMWF-66.011/0044-II/3b/2011 and BMWF-66.011/0059-II/3b/2011) and conformed to the Austrian guidelines on animal welfare and experimentation. All possible steps were taken to reduce suffering and the number of animals used during the experiment.

5.2. Win-shift acquisition using an eight-arm radial maze

Spatial learning and memory were assessed using a modified win-shift procedure in a baited 8-arm radial maze (PanLab, Spain) as previously described by us (Pirchl et al., 2010; Ullrich et al., 2010). The maze consisted of a central starting arena from which eight identical Plexiglas arms radiated. Cups were placed at the ends of each arm where water could be placed as a reward (bait). To facilitate spatial navigation, small high contrast visual cues were placed above the entrance to four arms. To exclude olfactory interference, the maze apparatus was cleaned with 70% ethanol following each trial. To rule out analysis bias, investigators were blinded to the condition of the mice. The behavioral test equipment was automatically controlled and monitored by a computer equipped with Mazesoft 8.1.9 Software.

In order to acclimatize animals to the apparatus and experimental set-up, animals were given 4 training sessions on day 1 and then placed on water restriction overnight to increase motivation for finding water (baits). On day 2, prior to behavioral testing, all arms were baited with 30 µl of water and mice were given 5 min to explore the maze. Animals were tested on day 2 for spatial learning abilities with eight consecutive sessions and then placed back on normal water consumption. For retention (memory) trials, animals were placed on water restriction overnight on day 7 and then tested the following day (day 8) with two sessions (at least 1 h apart). Quantification of cognitive performance (spatial learning and memory) was done by calculating the number of working memory errors made and the entries to repeat measure. Working memory errors involve the animal re-entering an arm that was already visited. The entries to repeat measure captures choice accuracy and is defined by the number of correct entries into baited arms until an error is made.

5.3. Plasma and tissue collection

At the end of the experiment, animals were anesthetized by subcutaneous sodium thiopental (12.5 mg/ml, 1 ml) injection. Blood was taken directly from the heart, collected in EDTA tubes, and centrifuged at 400 ×*g* for 10 min. Plasma was stored at −80 °C until further use. Immediately after taking the blood, a transcardial perfusion was performed with 20 ml of phosphate-buffered saline solution (PBS) containing EDTA and heparin and then subsequently with 50 ml of 4% paraformaldehyde (PFA) in PBS. The brain was removed, post-fixed in 4% PFA for 3 h at 4 °C, and then immersed in a 20% sucrose/PBS solution overnight. A medial sagittal cut was made to divide the brain into the 2 hemispheres and then stored in 0.1% sodium azide/PBS solution until further use. The left hemisphere was used for immunohistochemical evaluations and the right hemisphere was used for MRI imaging.

5.4. Corticosterone ELISA

Plasma corticosterone levels were measured using the ACE™ Corticosterone EIA kit (Cayman Chemical, Item No. 500655) according to the manufacturer's instructions. Briefly, 50 µl of each standard and sample was added to the provided plate and incubated with 50 µl of Corticosterone AChE Tracer and 50 µl of Corticosterone EIA Antiserum for 2 h at room temperature shaking. Following this, the plate was washed five times with 350 µl of Wash Buffer. For development, 200 µl of Ellman's Reagent was added to each well and incubated for 90 min in the dark shaking. Signal absorbance was measured at 405 nm by an ELISA plate reader (Zenyth 3100). The concentration of each sample was quantified according to the manufacturer's instructions using the provided Cayman spreadsheet and data analysis tool, plotting %Bound/Maximum Bound ($\%B/B_0$) for standards versus corticosterone log concentration using a four-parametric logistic fit.

5.5. Plasma cholesterol levels

Plasma cholesterol levels were analyzed using HPLC and UV detection (Shimadzu) as previously described by us (Ullrich et al., 2010). Briefly, 60 µl of plasma was mixed with 1 ml of alcoholic potassium hydroxide and incubated for 30 min at 75 °C. After cooling to room temperature, 1 ml of de-ionized water and 2 ml of n-hexane were added to the samples. The samples were then agitated for 15 min and centrifuged for 5 min at 200 ×*g*. One mililiter of the n-hexane (upper) layer was transferred into a glass tube and evaporated at 75 °C. Residues were dissolved in 150 µl of mobile phase (44% acetonitrile, 54% isopropanol, 2% dH_2O) and 100 µl was injected onto the column (Nucleosil 120-5 C18, 250 × 4.6 mm) with a flow of 0.6 ml/min. Cholesterol was observed at 205 nm using a UV-detector (Shimadzu). Sample values were calculated from a standard curve in the linear range.

5.6. Immunohistochemistry

Brain sections were evaluated immunohistochemically at 7, 14 and 20 months of age (i.e. 5, 12, and 18 months after beginning the special diet regimen). Immunohistochemistry was performed as previously described under free-floating conditions (Hohsfield et al., 2013; Pirchl et al., 2010; Ullrich et al., 2010). The right brain hemisphere was placed on a cork, frozen in a CO_2 stream and subsequently cut into 40-µm cryostat (Leica CM 1950) sections. The brain sections were then washed with PBS and incubated in PBS/0.1% Triton (T-PBS) for 30 min at 20 °C while shaking. To quench endogenous peroxidase, sections were treated with PBS/1%H_2O_2/5% methanol. After incubation, the sections were then blocked in T-PBS/20% horse serum (GIBCO Invitrogen)/0.2% BSA (SERVA) for 30 min at 20 °C shaking. Following blocking, brain sections were incubated with primary antibody (Table 1) in T-PBS/0.2% BSA overnight at 20 °C. The sections were then washed and incubated with the corresponding biotinylated secondary antibody (1:200, Vector Laboratories) in T-PBS/0.2% BSA for 1 h at 20 °C shaking. To evaluate BBB permeability, some sections were also incubated with biotinylated rabbit anti-mouse IgG (1:400, Vector) as previously described for rats (Pirchl et al., 2010; Ullrich et al., 2010). Following secondary antibody incubation, sections were rinsed with PBS and incubated in avidin-biotin complex solution (Elite ABC kit, Vector Laboratories) for 1 h at 20 °C shaking. Finally, the sections were washed with 50

mM Tris-buffered saline (TBS) and then incubated in 0.5 mg/ml 3,3′-diaminobenzidine (DAB, Sigma)/TBS/0.003% H_2O_2 at 20 °C in the dark until a signal was detected. Once DAB staining was visible, the reaction was stopped by adding TBS to the sections. The brain sections were rinsed with TBS, mounted onto glass slides, cover-slipped with Entellan (Merck, Darmstadt, Germany), and then evaluated under the microscope by a blinded investigator.

5.7. MRI analysis

The brains from WT and 3xTg-AD mice fed a normal or cholesterol diet were scanned at 7, 14, and 20 months of age, as well as brains from 6- and 12-month-old APPSwDI mice. MRI was performed using a 9.4 T Bruker 94/20 BioSpec equipped with a BGA12S or BGA12S-HP gradient system (Bruker, Ettlingen, Germany). The gradient system was replaced after 7- and 14-month-old brains had been scanned. Proton imaging was performed on perfused brains using a proton 89/23 mm quadrupolar volume coil and Paravision software 5.1 (Bruker). Each brain was divided sagittally at the midline, immersed in Fomblin oil, to decrease the background, and suspended in a 2 ml syringe. An axial T2* FLASH sequence was used with TR/TE = 701/20 ms, slice thickness = 0.5 mm with no interslice distance, flip angel = 35°, matrix = 96x96, number of averages = 100, field of view = 7.5 × 7.5 mm, and 1st and 2nd order shims were adjusted before the scan was performed. The scans were post-processed with susceptibility weighted imaging (SWI) module (Bruker) with processing parameters negative, mark weighting mode, mask weighting = 10.00 and Gauss Broadening = 2.00 to enhance detection of microbleedings.

5.8. Microscopic evaluations

Images were captured with an Olympus BX61 (ProgRes C14 camera) microscope equipped with Openlab 5.5.0 imaging software. For quantification, two to four brain sections per animal were evaluated for cortical staining patterns. The number of Aβ-positive neurons, vessels or tau-positive neurons/tangles per cortex was quantified under 10× or 20× objectives by a blind observer. Semi-quantitative analysis of hippocampal IgG and ApoE staining was also performed using the following scheme: 0 = no staining, 1 = little staining, 2 = some staining, 3 = moderate staining, 4 = heavy staining, and 5 = severe staining deposition. Collagen IV staining was evaluated using ImageJ optical density (O.D.) analysis and the Analyze Skeleton plugin (Arganda-Carreras et al., 2010) to measure number of vessel branches and average vessel branch length per 20× section (field size).

5.9. Statistical analysis

All data are reported as mean ± SEM (n = independent experiments or individual animals). Differences between mean values were determined using the Student’s t-test, one-way ANOVA followed by a Fisher least significant difference post hoc test, or two-way ANOVA followed by Bonferroni post hoc test with time and genotype as the two factors for MRI analysis. The area of the lateral ventricle was measured using Paravision software at the level of bregma. p values < 0.05 were considered significant.

Acknowledgments

This study has been supported by the Austrian Science Fund (P24734-B24) and the Swedish Research Council (09917). We thank Ursula Kirzenberger-Winkler for her excellent technical assistance.

References

Arganda-Carreras I, Fernandez-Gonzalez R, Munoz-Barrutia A, Ortiz-De-Solorzano C. 3D reconstruction of histological sections: application to mammary gland tissue. Microsc. Res. Tech. 2010; 73:1019–1029. [PubMed: 20232465]

Beckmann N, Gerard C, Abramowski D, Cannet C, Staufenbiel M. Noninvasive magnetic resonance imaging detection of cerebral amyloid angiopathy-related microvascular alterations using superparamagnetic iron oxide particles in APP transgenic mouse models of Alzheimer's disease: application to passive Abeta immunotherapy. J. Neurosci. Off. J. Soc. Neurosci. 2011; 31:1023–1031.

Bedrosian TA, Herring KL, Weil ZM, Nelson RJ. Altered temporal patterns of anxiety in aged and amyloid precursor protein (APP) transgenic mice. Proc. Natl. Acad. Sci. U. S. A. 2011; 108:11686–11691. [PubMed: 21709248]

Beel AJ, Sakakura M, Barrett PJ, Sanders CR. Direct binding of cholesterol to the amyloid precursor protein: an important interaction in lipid-Alzheimer's disease relationships? Biochim. Biophys. Acta. 2010; 1801:975–982. [PubMed: 20304095]

Bertram L, Lill CM, Tanzi RE. The genetics of Alzheimer disease: back to the future. Neuron. 2010; 68:270–281. [PubMed: 20955934]

Billings LM, Oddo S, Green KN, McGaugh JL, LaFerla FM. Intraneuronal Abeta causes the onset of early Alzheimer's disease-related cognitive deficits in transgenic mice. Neuron. 2005; 45:675–688. [PubMed: 15748844]

Bourasset F, Ouellet M, Tremblay C, Julien C, Do TM, Oddo S, LaFerla F, Calon F. Reduction of the cerebrovascular volume in a transgenic mouse model of Alzheimer's disease. Neuropharmacology. 2009; 56:808–813. [PubMed: 19705573]

Bu G. Apolipoprotein E and its receptors in Alzheimer's disease: pathways, pathogenesis and therapy. Nat. Rev. Neurosci. 2009; 10:333–344. [PubMed: 19339974]

Chen CC, Tung YY, Chang C. A lifespan MRI evaluation of ventricular enlargement in normal aging mice. Neurobiol. Aging. 2011; 32:2299–2307. [PubMed: 20137831]

Darwish DS, Wang D, Konat GW, Schreurs BG. Dietary cholesterol impairs memory and memory increases brain cholesterol and sulfatide levels. Behav. Neurosci. 2010; 124:115–123. [PubMed: 20141286]

Davis J, Xu F, Deane R, Romanov G, Previti ML, Zeigler K, Zlokovic BV, Van Nostrand WE. Early-onset and robust cerebral microvascular accumulation of amyloid beta-protein in transgenic mice expressing low levels of a vasculotropic Dutch/Iowa mutant form of amyloid beta-protein precursor. J. Biol. Chem. 2004; 279:20296–20306. [PubMed: 14985348]

de la Torre JC. Vascular risk factors: a ticking time bomb to Alzheimer's disease. Am. J. Alzheimers Dis. Other Demen. 2013; 28:551–559. [PubMed: 23813612]

De Reuck J, Deramecourt V, Cordonnier C, Leys D, Pasquier F, Maurage CA. Prevalence of small cerebral bleeds in patients with a neurodegenerative dementia: a neuropathological study. J. Neurol. Sci. 2011; 300:63–66. [PubMed: 20965516]

Deci S, Lemieux SK, Smith-Bell CA, Sparks DL, Schreurs BG. Cholesterol increases ventricular volume in a rabbit model of Alzheimer's disease. J. Alzheimers Dis. 2012; 29:283–292. [PubMed: 22232012]

Di Paolo G, Kim TW. Linking lipids to Alzheimer's disease: cholesterol and beyond. Nat. Rev. Neurosci. 2011; 12:284–296. [PubMed: 21448224]

Filiano AJ, Tucholski J, Dolan PJ, Colak G, Johnson GV. Transglutaminase 2 protects against ischemic stroke. Neurobiol. Dis. 2010; 39:334–343. [PubMed: 20451610]

Gama Sosa MA, Gasperi RD, Rocher AB, Wang AC, Janssen WG, Flores T, Perez GM, Schmeidler J, Dickstein DL, Hof PR, et al. Age-related vascular pathology in transgenic mice expressing

presenilin 1-associated familial Alzheimer's disease mutations. Am. J. Pathol. 2010; 176:353–368. [PubMed: 20008141]

Gamba P, Testa G, Sottero B, Gargiulo S, Poli G, Leonarduzzi G. The link between altered cholesterol metabolism and Alzheimer's disease. Ann. N. Y. Acad. Sci. 2012; 1259:54–64. [PubMed: 22758637]

Ghribi O. Potential mechanisms linking cholesterol to Alzheimer's disease-like pathology in rabbit brain, hippocampal organotypic slices, and skeletal muscle. J. Alzheimers Dis. 2008; 15:673–684. [PubMed: 19096164]

Ghribi O, Golovko MY, Larsen B, Schrag M, Murphy EJ. Deposition of iron and beta-amyloid plaques is associated with cortical cellular damage in rabbits fed with long-term cholesterol-enriched diets. J. Neurochem. 2006; 99:438–449. [PubMed: 17029598]

Goymann W, Möstl E, Gwinner E, Karasov WH. Corticosterone metabolites can be measured noninvasively in excreta of European stonechats (*Saxicola torquata rubicol*a). Auk. 2002; 119:1167–1173.

Grammas P, Martinez J, Sanchez A, Yin X, Riley J, Gay D, Desobry K, Tripathy D, Luo J, Evola M, et al. A new paradigm for the treatment of Alzheimer's disease: targeting vascular activation. J. Alzheimers Dis. 2014; 40:619–630. [PubMed: 24503617]

Granholm AC, Bimonte-Nelson HA, Moore AB, Nelson ME, Freeman LR, Sambamurti K. Effects of a saturated fat and high cholesterol diet on memory and hippocampal morphology in the middle-aged rat. J. Alzheimers Dis. 2008; 14:133–145. [PubMed: 18560126]

Grinberg LT, Thal DR. Vascular pathology in the aged human brain. Acta Neuropathol. 2010; 119:277–290. [PubMed: 20155424]

Haag MD, Hofman A, Koudstaal PJ, Stricker BH, Breteler MM. Statins are associated with a reduced risk of Alzheimer disease regardless of lipophilicity. The Rotterdam Study. J. Neurol. Neurosurg. Psychiatry. 2009; 80:13–17. [PubMed: 18931004]

Hardy J, Selkoe DJ. The amyloid hypothesis of Alzheimer's disease: progress and problems on the road to therapeutics. Science. 2002; 297:353–356. [PubMed: 12130773]

Herzig MC, Winkler DT, Burgermeister P, Pfeifer M, Kohler E, Schmidt SD, Danner S, Abramowski D, Sturchler-Pierrat C, Burki K, et al. Abeta is targeted to the vasculature in a mouse model of hereditary cerebral hemorrhage with amyloidosis. Nat. Neurosci. 2004; 7:954–960. [PubMed: 15311281]

Hirata-Fukae C, Li HF, Hoe HS, Gray AJ, Minami SS, Hamada K, Niikura T, Hua F, Tsukagoshi-Nagai H, Horikoshi-Sakuraba Y, et al. Females exhibit more extensive amyloid, but not tau, pathology in an Alzheimer transgenic model. Brain Res. 2008; 1216:92–103. [PubMed: 18486110]

Hohsfield LA, Ehrlich D, Humpel C. Cholesterol diet counteracts repeated anesthesia/infusion-induced cognitive deficits in male Brown Norway rats. Neurobiol. Learn. Mem. 2013; 106C:154–162. [PubMed: 23973449]

Humpel C. Chronic mild cerebrovascular dysfunction as a cause for Alzheimer's disease? Exp. Gerontol. 2011; 46:225–232. [PubMed: 21112383]

Hunter JM, Bowers WJ, Maarouf CL, Mastrangelo MA, Daugs ID, Kokjohn TA, Kalback WM, Luehrs DC, Valla J, Beach TG, et al. Biochemical and morphological characterization of the AbetaPP/PS/tau triple transgenic mouse model and its relevance to sporadic Alzheimer's disease. J. Alzheimers Dis. 2011; 27:361–376. [PubMed: 21860086]

Iadecola C. The pathobiology of vascular dementia. Neuron. 2013; 80:844–866. [PubMed: 24267647]

Jones L, Holmans PA, Hamshere ML, Harold D, Moskvina V, Ivanov D, Pocklington A, Abraham R, Hollingworth P, Sims R, et al. Genetic evidence implicates the immune system and cholesterol metabolism in the aetiology of Alzheimer's disease. PLoS One. 2010; 5:e13950. [PubMed: 21085570]

Knight EM, Martins IV, Gumusgoz S, Allan SM, Lawrence CB. High-fat diet-induced memory impairment in triple-transgenic Alzheimer's disease (3xTgAD) mice is independent of changes in amyloid and tau pathology. Neurobiol. Aging. 2014; 35:1821–1832. [PubMed: 24630364]

Kumar-Singh S, Pirici D, McGowan E, Serneels S, Ceuterick C, Hardy J, Duff K, Dickson D, Van Broeckhoven C. Dense-core plaques in Tg2576 and PSAPP mouse models of Alzheimer's disease are centered on vessel walls. Am. J. Pathol. 2005; 167:527–543. [PubMed: 16049337]

Lambert JC, Ibrahim-Verbaas CA, Harold D, Naj AC, Sims R, Bellenguez C, Jun G, Destefano AL, Bis JC, Beecham GW, et al. Meta-analysis of 74,046 individuals identifies 11 new susceptibility loci for Alzheimer's disease. Nat. Genet. 2013; 45:1452–1458. [PubMed: 24162737]

Maulik M, Westaway D, Jhamandas JH, Kar S. Role of cholesterol in APP metabolism and its significance in Alzheimer's disease pathogenesis. Mol. Neurobiol. 2013; 47:37–63. [PubMed: 22983915]

Nestor SM, Rupsingh R, Borrie M, Smith M, Accomazzi V, Wells JL, Fogarty J, Bartha R. Ventricular enlargement as a possible measure of Alzheimer's disease progression validated using the Alzheimer's disease neuroimaging initiative database. Brain. 2008; 131:2443–2454. [PubMed: 18669512]

Oddo S, Caccamo A, Shepherd JD, Murphy MP, Golde TE, Kayed R, Metherate R, Mattson MP, Akbari Y, LaFerla FM. Triple-transgenic model of Alzheimer's disease with plaques and tangles: intracellular Abeta and synaptic dysfunction. Neuron. 2003; 39:409–421. [PubMed: 12895417]

Perez-Garmendia R, Hernandez-Zimbron LF, Morales MA, Luna-Munoz J, Mena R, Nava-Catorce M, Acero G, Vasilevko V, Viramontes-Pintos A, Cribbs DH, et al. Identification of N-terminally truncated pyroglutamate amyloid-beta in cholesterol-enriched diet-fed rabbit and AD brain. J. Alzheimers Dis. 2014; 39:441–455. [PubMed: 24240639]

Petanceska SS, DeRosa S, Sharma A, Diaz N, Duff K, Tint SG, Refolo LM, Pappolla M. Changes in apolipoprotein E expression in response to dietary and pharmacological modulation of cholesterol. J. Mol. Neurosci. 2003; 20:395–406. [PubMed: 14501024]

Philipson O, Lord A, Gumucio A, O'Callaghan P, Lannfelt L, Nilsson LN. Animal models of amyloid-beta-related pathologies in Alzheimer's disease. FEBS J. 2010; 277:1389–1409. [PubMed: 20136653]

Pirchl M, Ullrich C, Humpel C. Differential effects of short- and long-term hyperhomocysteinaemia on cholinergic neurons, spatial memory and microbleedings in vivo in rats. Eur. J. Neurosci. 2010; 32:1516–1527. [PubMed: 21044172]

Puglielli L, Tanzi RE, Kovacs DM. Alzheimer's disease: the cholesterol connection. Nat. Neurosci. 2003; 6:345–351. [PubMed: 12658281]

Querfurth HW, LaFerla FM. Alzheimer's disease. N. Engl. J. Med. 2010; 362:329–344. [PubMed: 20107219]

Raber J. Role of apolipoprotein E in anxiety. Neural Plast. 2007; 2007:91236. [PubMed: 17710250]

Ramesh BN, Raichurkar KP, Shamasundar NM, Rao TS, Rao KS. Abeta(42) induced MRI changes in aged rabbit brain resembles AD brain. Neurochem. Int. 2011; 59:637–642. [PubMed: 21723897]

Refolo LM, Malester B, LaFrancois J, Bryant-Thomas T, Wang R, Tint GS, Sambamurti K, Duff K, Pappolla MA. Hypercholesterolemia accelerates the Alzheimer's amyloid pathology in a transgenic mouse model. Neurobiol. Dis. 2000; 7:321–331. [PubMed: 10964604]

Reiss AB, Voloshyna I. Regulation of cerebral cholesterol metabolism in Alzheimer disease. J. Investig. Med. 2012; 60:576–582.

Sagare AP, Bell RD, Zlokovic BV. Neurovascular defects and faulty amyloid-beta vascular clearance in Alzheimer's disease. J. Alzheimers Dis. 2013; 33(Suppl 1):S87–S100. [PubMed: 22751174]

Schreurs BG. The effects of cholesterol on learning and memory. Neurosci. Biobehav. Rev. 2010; 34:1366–1379. [PubMed: 20470821]

Schreurs BG, Wang D, Smith-Bell CA, Burhans LB, Bell R, Gonzalez-Joekes J. Dietary cholesterol concentration and duration degrade long-term memory of classical conditioning of the rabbit's nictitating membrane response. Int. J. Alzheimers Dis. 2012; 2012:732634. [PubMed: 22567532]

Schreurs BG, Smith-Bell CA, Wang D, Burhans LB. Dietary cholesterol degrades rabbit long term memory for discrimination learning but facilitates acquisition of discrimination reversal. Neurobiol. Learn. Mem. 2013; 106:238–245. [PubMed: 24076265]

Shobab LA, Hsiung GY, Feldman HH. Cholesterol in Alzheimer's disease. Lancet Neurol. 2005; 4:841–852. [PubMed: 16297842]

Sparks DL, Kuo YM, Roher A, Martin T, Lukas RJ. Alterations of Alzheimer's disease in the cholesterol-fed rabbit, including vascular inflammation. Preliminary observations. Ann. N. Y. Acad. Sci. 2000; 903:335–344. [PubMed: 10818523]

Sterniczuk R, Antle MC, Laferla FM, Dyck RH. Characterization of the 3xTg-AD mouse model of Alzheimer's disease: part 2. Behavioral and cognitive changes. Brain Res. 2010; 1348:149–155. [PubMed: 20558146]

Thirumangalakudi L, Prakasam A, Zhang R, Bimonte-Nelson H, Sambamurti K, Kindy MS, Bhat NR. High cholesterol-induced neuroinflammation and amyloid precursor protein processing correlate with loss of working memory in mice. J. Neurochem. 2008; 106:475–485. [PubMed: 18410513]

Ullrich C, Pirchl M, Humpel C. Hypercholesterolemia in rats impairs the cholinergic system and leads to memory deficits. Mol. Cell. Neurosci. 2010; 45:408–417. [PubMed: 20696249]

Umeda T, Tomiyama T, Kitajima E, Idomoto T, Nomura S, Lambert MP, Klein WL, Mori H. Hypercholesterolemia accelerates intraneuronal accumulation of Abeta oligomers resulting in memory impairment in Alzheimer's disease model mice. Life Sci. 2012; 91:1169–1176. [PubMed: 22273754]

Wilhelmus MM, de Jager M, Drukarch B. Tissue transglutaminase: a novel therapeutic target in cerebral amyloid angiopathy. Neurodegener. Dis. 2012; 10:317–319. [PubMed: 22156619]

Wood WG, Li L, Muller WE, Eckert GP. Cholesterol as a causative factor in Alzheimer's disease: a debatable hypothesis. J. Neurochem. 2014; 129:559–572. [PubMed: 24329875]

Xie Z, Yang D, Stephenson D, Morton D, Hicks C, Brown T, Bocan T. Characterizing the regional structural difference of the brain between tau transgenic (rTg4510) and wild-type mice using MRI. Med. Image Comput. Comput. Assist. Interv. 2010; 13:308–315. [PubMed: 20879245]

Xue QS, Sparks DL, Streit WJ. Microglial activation in the hippocampus of hypercholesterolemic rabbits occurs independent of increased amyloid production. J. Neuroinflammation. 2007; 4:20. [PubMed: 17718905]

Zlokovic BV. The blood–brain barrier in health and chronic neurodegenerative disorders. Neuron. 2008; 57:178–201. [PubMed: 18215617]

Europe PMC Funders Author Manuscripts

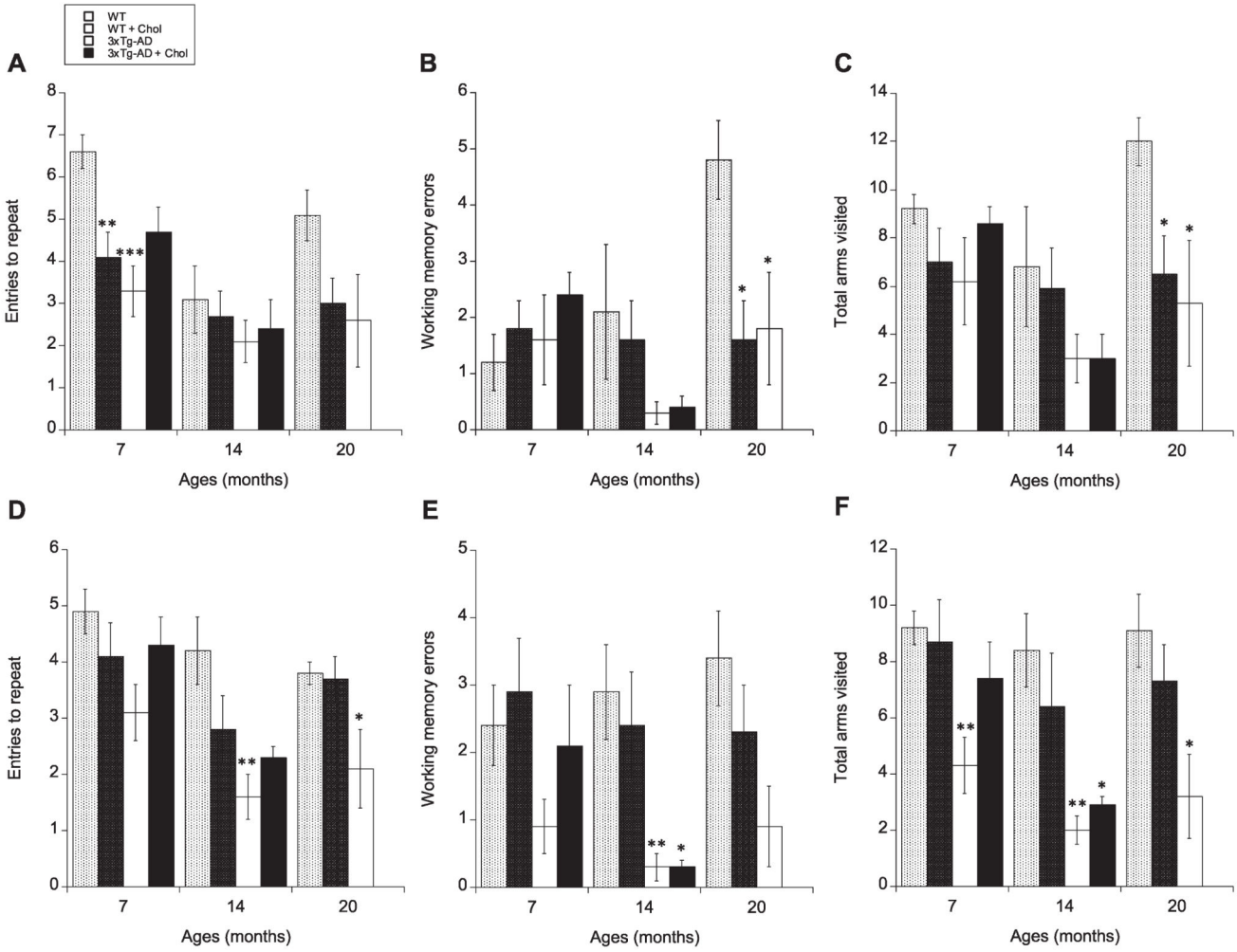

Fig. 1.

Effects of high cholesterol diet on learning (A–C) and memory (E–F). Spatial memory (A–C) and learning (D–F) using the win-shift procedure in a baited 8-arm radial maze were evaluated in wildtype (WT) and triple-transgenic AD (3xTg-AD) animals fed a normal or 5% cholesterol diet for 7, 14, and 20 months. Memory and learning were assessed by the number of entries to repeat (A & D) and working memory errors (B & E). The number of total arms visited was also evaluated as an internal control (C & F). Memory was tested one week following learning assessment. Values represent mean visits or errors ± SEM. Five animals were examined per group. Statistical analysis was performed using a multivariate and/or one-way ANOVA and Fisher's LSD posthoc test. Symbols indicate the significant difference between groups compared to WT (*$p < 0.05$, **$p < 0.01$, *** $p < 0.001$).

Europe PMC Funders Author Manuscripts

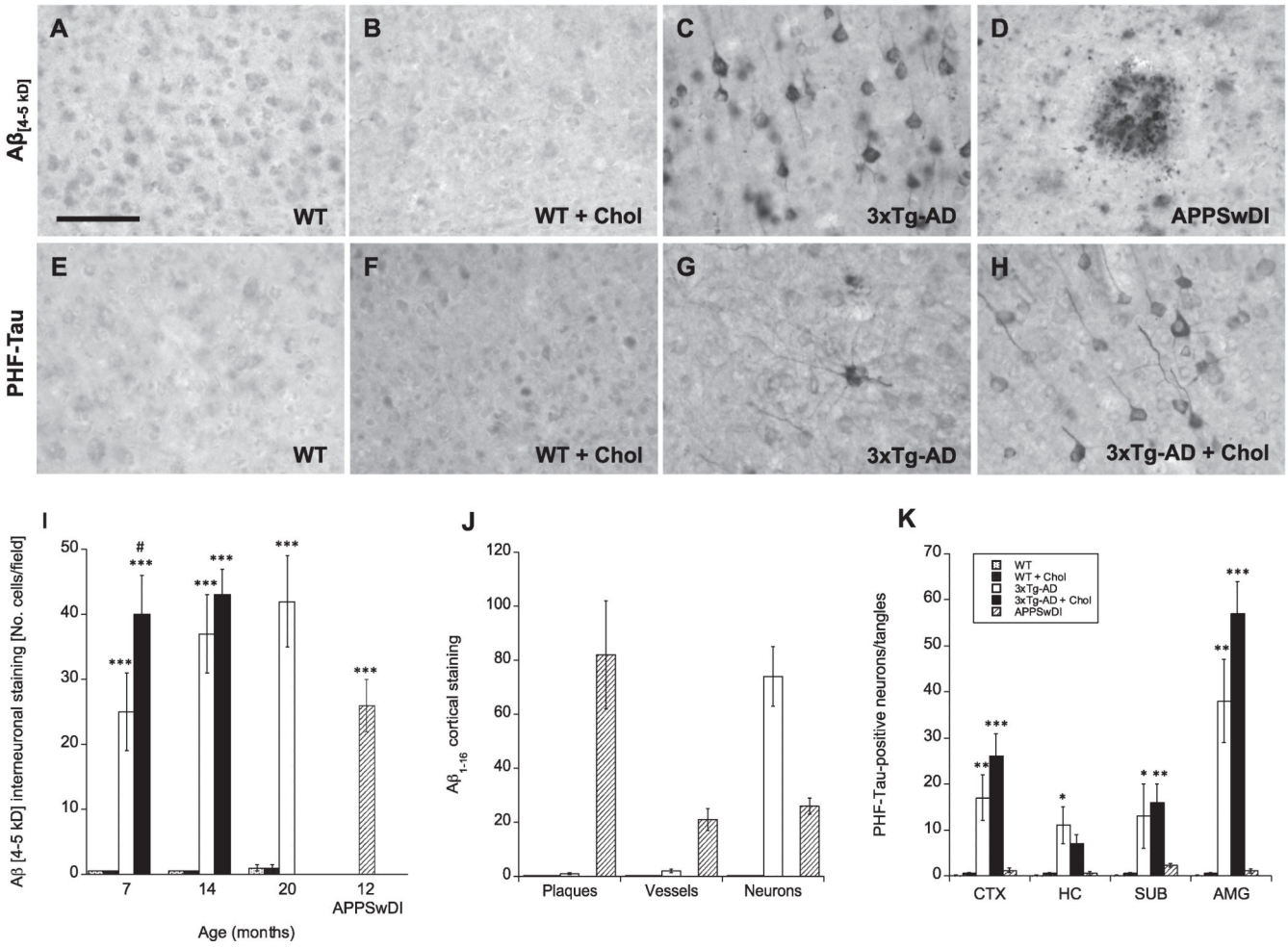

Fig. 2.

Effects of high cholesterol diet on β-amyloid and tau pathology in wildtype (WT) and triple-transgenic (3xTg) AD mice. Wildtype (WT; A, B, E, F) and triple-transgenic AD (3xTg-AD; C, G, H) mice were fed a normal (A, C, E, G) or 5% cholesterol diet (B, F, H) for 7, 14, and 20 months. APPSwDI mice (12-month-old) were used as a positive control for plaque deposition (D). At different time points, brains were collected, sectioned (40 μm), and stained for β-amyloid (Aβ 4–5 kD; A–D, I) or phospho-tau (E–H). Aβ-positive plaques were most prominent in APPSwDI mice (D). Phospho-tau neurons were visible in 3xTg-AD mice (G) and appeared enhanced by cholesterol diet (H). Images shown were taken from animals at 20 months of age, except for 3xTg-AD + Chol animals (H), which only survived up to 14 months. Quantitative analysis is shown for interneuronal Aβ 4–5 kD staining (I), Aβ 1–16 staining (J) and phospho-tau staining (K). Different treatments (bar labeling representing animal groups) are explained in panel K. Three to four brain sections were evaluated per animal. Values represent mean ± SEM. Five animals were examined per group. Statistical analysis was performed using a one-way ANOVA and Fisher's LSD posthoc test. Symbols indicate the significant difference between groups compared to WT (*$p < 0.05$, **$p < 0.01$, ***$p < 0.001$) or 3xTg-AD (#$p < 0.05$). Scale bar in A = 50 μm (A–H).

Europe PMC Funders Author Manuscripts

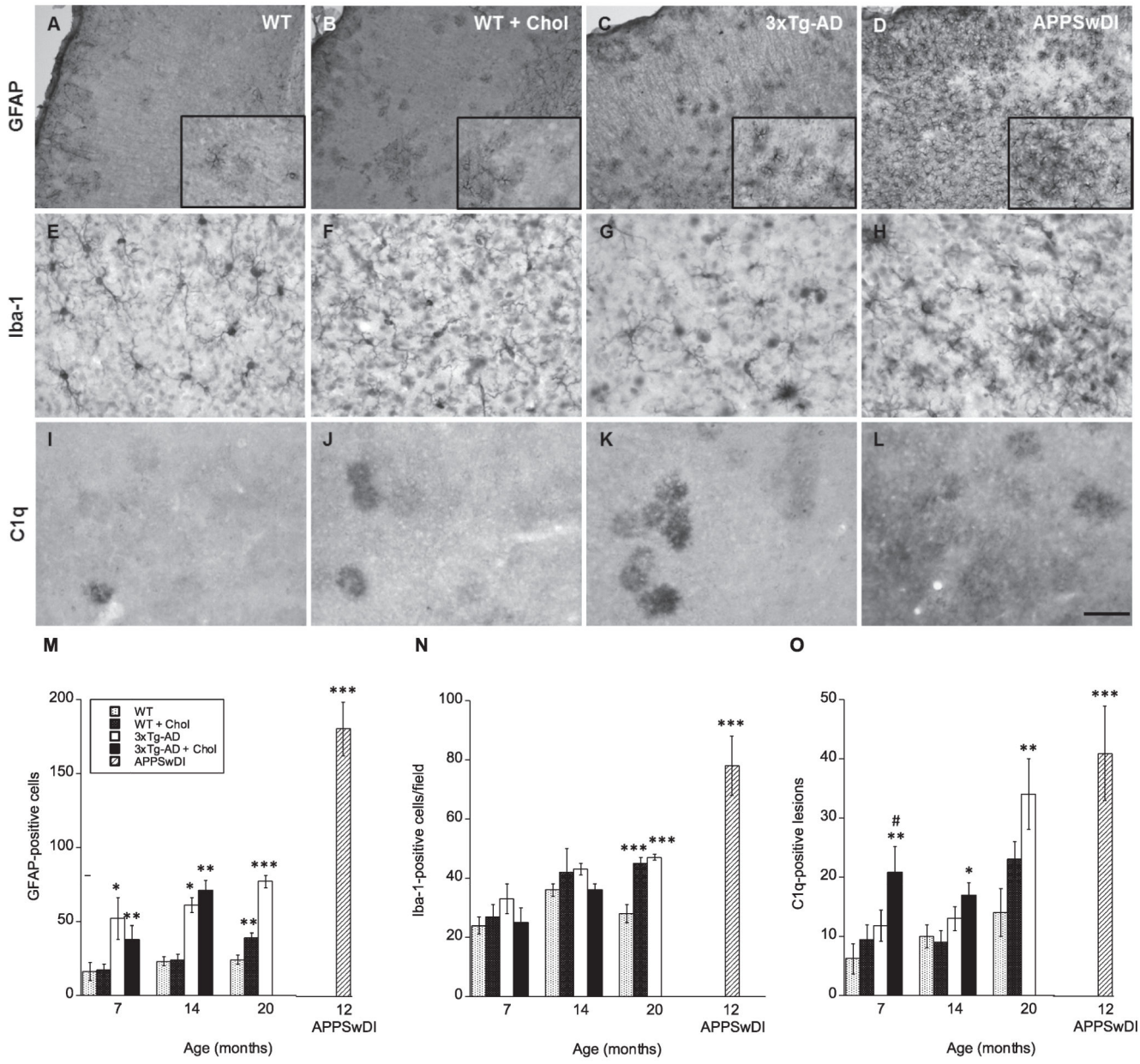

Fig. 3.

Effects of high cholesterol diet on neuroinflammation. Wildtype (WT) (A, E, I) and triple-transgenic AD (3xTg-AD; C, G, K) were fed a 5% cholesterol diet (B, F, J) for 7, 14, and 20 months. APPSwDI mice (12-month-old) were used as a positive control (D, H, L). At different time points, brains were collected, sectioned (40 μm), and stained for immune-related cells and components: astrocyte marker GFAP (A–D), microglia/macrophage marker Iba1 (E–H), and complement subcomponent C1q (I–L). Images shown were taken from animals at 20 months of age, except for APPSwDI animals (D, H, L), which were 12 months old. Quantitative analysis is shown for GFAP (M), Iba1 (N) and C1q (O). Different treatments (bar labeling) are explained in panel M. Three to four brain sections were evaluated per animal. Values represent mean number of cortical GFAP or Iba1-positive cells

or C1q lesions ± SEM. Five animals were examined per group. Statistical analysis was performed using a one-way ANOVA and Fisher's LSD posthoc test. Symbols indicate the significant difference between groups compared to WT (*p < 0.05, **p < 0.01, ***p < 0.001) or 3xTg-AD (#p < 0.05). Scale bar = 100 μm (E–L), 200 μm (A–D), and 140 μm (A–D insets).

Europe PMC Funders Author Manuscripts

Europe PMC Funders Author Manuscripts

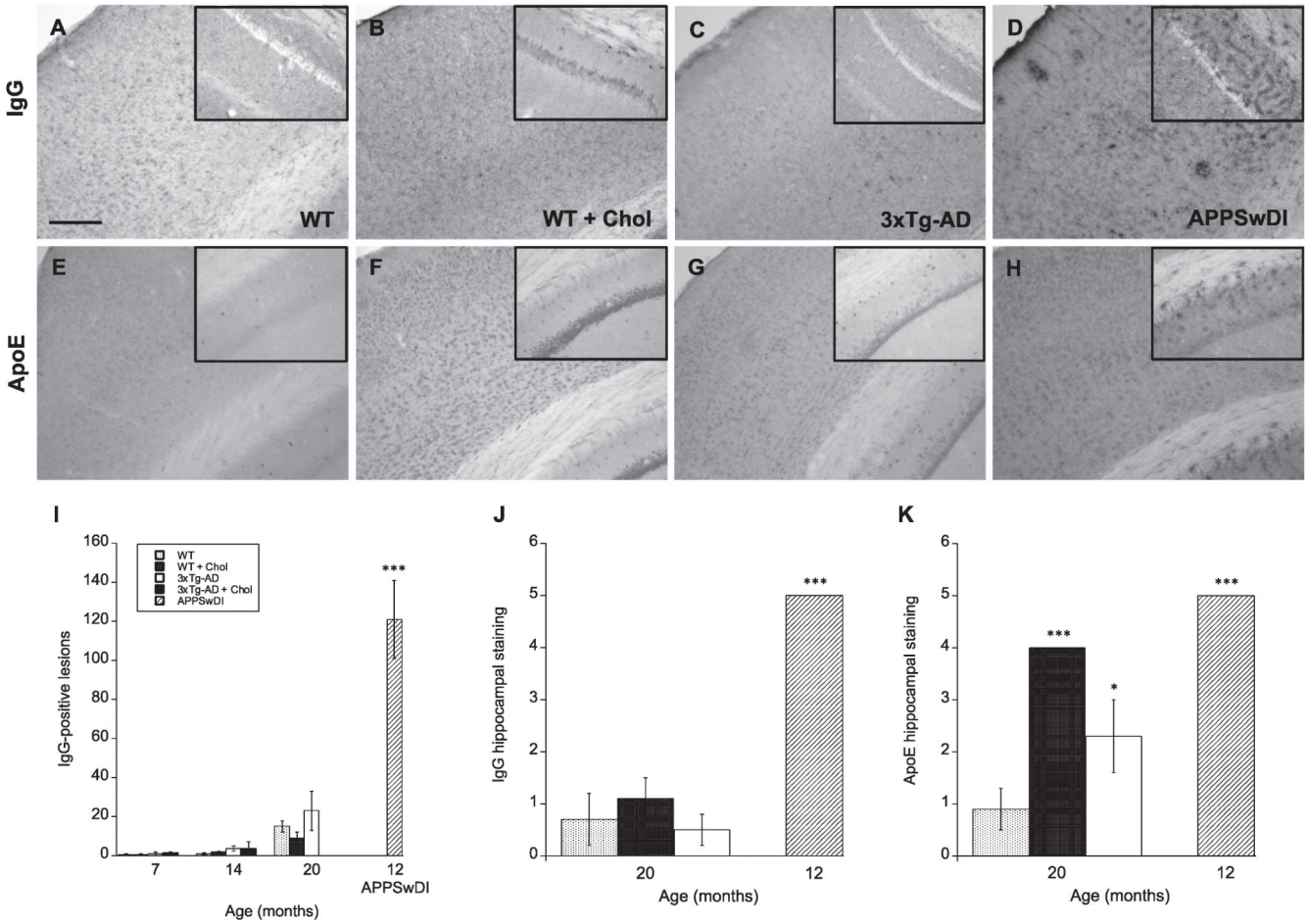

Fig. 4.

Plasma protein infiltration mice fed a high cholesterol diet. Wildtype (WT; A, B, E, F) and triple-transgenic AD (3xTg-AD; C & G) mice fed a 5% cholesterol diet (B & F) for 7, 14, and 20 months. APPSwDI mice (12-month-old) were used as a positive control (D & H). At different time points, blood–brain barrier disruption was evaluated by anti-mouse IgG staining (A-D) or apolipoprotein E (ApoE) immunoreactivity (E–H) in the cortex and hippocampus. Images shown were taken from animals at 20 months of age, unless otherwise indicated. Quantitative analysis is shown for anti-mouse IgG (I & J) or ApoE (K). Different treatments (bar labeling) are explained in panel I. Three to four brain sections were evaluated per animal. Values represent mean number of IgG lesions or IgG/ApoE semi-quantitative staining intensity ± SEM. Five animals were examined per group. Statistical analysis was performed using a one-way ANOVA and Fisher's LSD posthoc test. Symbols indicate the significant difference between groups compared to WT (*$p < 0.05$, ***$p < 0.001$). Scale bar = 100 μm (A–H) and 150 μm (A–H insets).

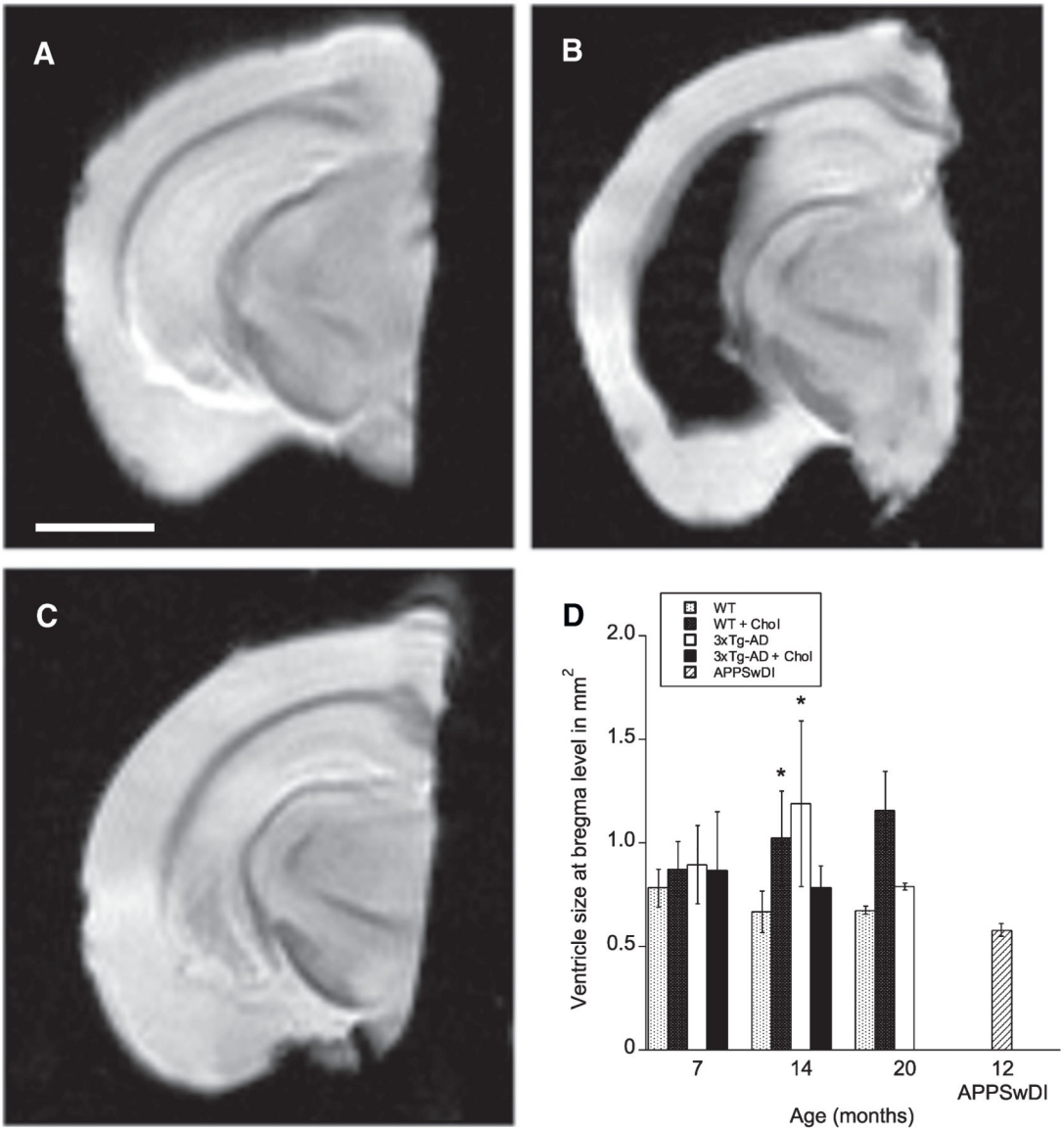

Fig. 5.

MRI detection of enlarged lateral ventricles. MRI analysis of lateral ventricle size was performed on wildtype (WT) and triple-transgenic (3xTg) AD animals fed a normal or 5% cholesterol diet for 7, 14, and 20 months. The lateral ventricles appeared normal in size in WT mice (A), while enlarged in 3xTg-AD mice (B) at 14 months of age at the hippocampal level. In APPSwDI mice no change in the size of the ventricles was apparent at 12 months of age (C). Unfortunately, Fomblin oil leaked into the enlarged ventricle in 3xTg-AD mice (B) turning it black, otherwise the ventricles appear white in the T2* sequence. Statistical analysis demonstrated that the genotypes ($F_{4, 61} = 3.267$, $p < 0.05$, two-way ANOVA), but not the time affected the lateral ventricle size at the level of bregma. The ventricles in APPSwDI were significantly smaller than WT cholesterol-fed and 3xTg-AD mice ($p < 0.05$) (D). Values represent mean ± SEM. Five animals were examined per group. Statistical analysis was performed using a two-way ANOVA and Bonferroni posthoc test. Symbols

indicate the significant difference between groups compared to WT (*$p < 0.05$). Scale bar in A = 1.7 mm (A–C).

Europe PMC Funders Author Manuscripts

Europe PMC Funders Author Manuscripts

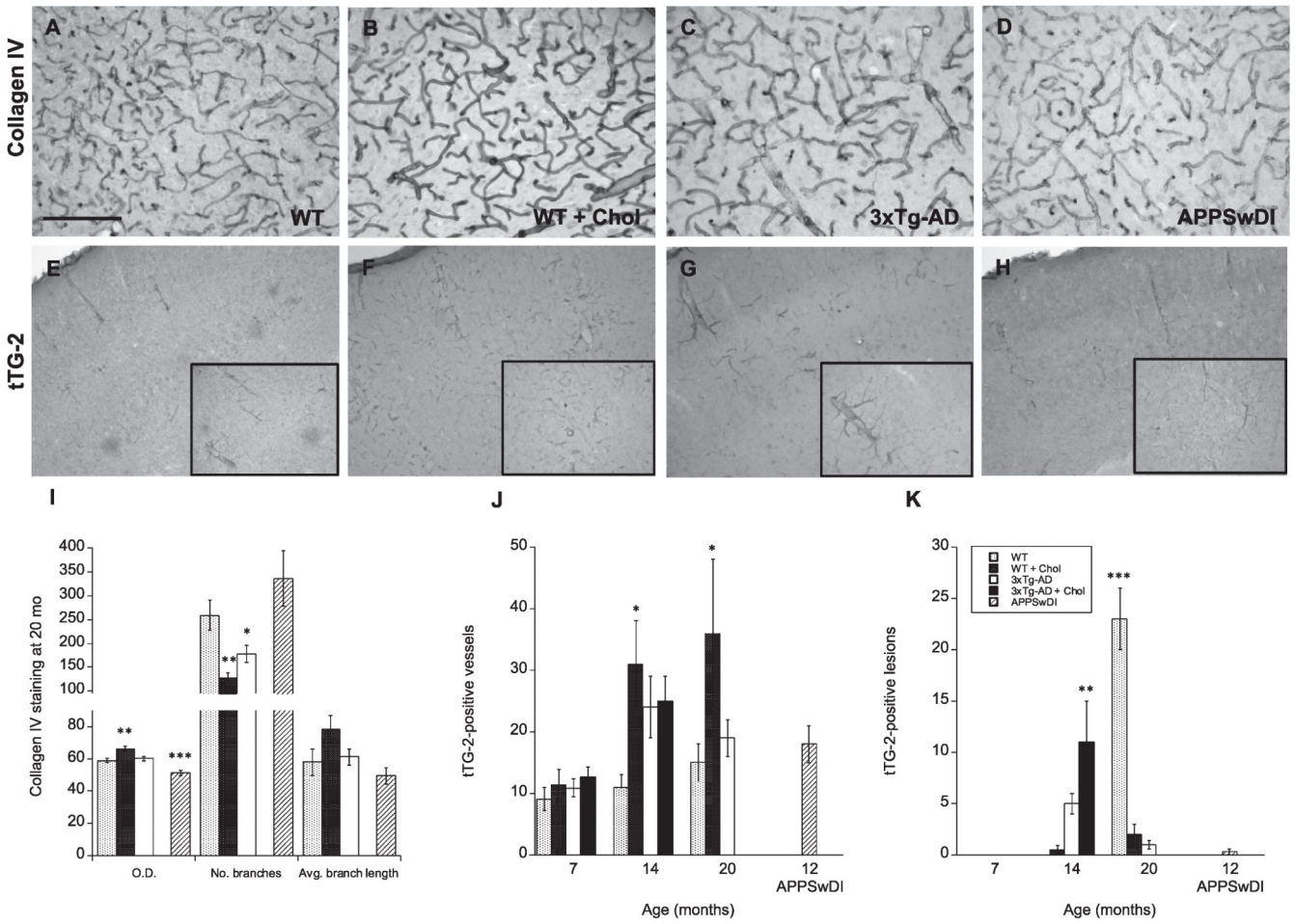

Fig. 6.

Vascular pathology in mice fed a high cholesterol diet. Wildtype (WT) (A & E), triple-transgenic 3xTg (C & G), WT mice fed with a 5% cholesterol diet (B & F) and 3xTg-AD mice fed with a 5% cholesterol diet (not shown) were analyzed at 7, 14, and 20 months. APPSwDI mice (12-month-old) were used as a positive control (D & H). Blood vessel morphology and vascular pathology were assessed using collagen IV (A–D) and transglutaminase-2 (tTG-2, E–H) staining. Quantitative analysis is shown for anti-mouse Collagen IV (I) or tTG-2 (J & K). Different treatments (bar labeling) are explained in panel K. Three to four brain sections were evaluated per animal. Values represent mean O.D., vessel branches or length, or vessels or lesions ± SEM. Five animals were examined per group. Statistical analysis was performed using a one-way ANOVA and Fisher's LSD posthoc test. Symbols indicate the significant difference between groups compared to WT (*$p < 0.05$, **$p < 0.01$, ***$p < 0.001$). Scale bar = 100 μm (A–D), 200 μm (E–H) and 80 μm (E–H insets).

Europe PMC Funders Author Manuscripts

Table 1

Primary antibodies for immunohistochemical evaluations.

Antibody	Company, Cat. No.	Dilution	Secondary
Aβ [4–5 kD]	Invitrogen, 71–5800	1:200	Rabbit
Aβ [13–28]	Sigma, A8978	1:250	Mouse
Aβ [1–16] (6E10)	Covance, SIG–39300	1:1000	Mouse
Apolipoprotein E (ApoE)	Abcam, ab1906	1:250	Mouse
C1q (biotinylated)	Thermo, MA1–40312	1:250	–
Collagen IV	Abcam, ab6586	1:500	Rabbit
Glial Fibrillary Acidic Protein (GFAP)	Millipore, AB5541	1:2000	Chicken
Iba1	Wako, 019–19741	1:500	Rabbit
Phospho-PHF-tau	Thermo, MN1020	1:1000	Mouse
Transglutaminase-2	Abcam, ab421	1:250	Rabbit

Europe PMC Funders Author Manuscripts

Table 2

Effects of cholesterol diet on animal weight.

Group	7 months	14 months	20 months
WT	31.7 ± 0.6 (5) -	37.9 ± 1.6 (5) -	35.7 ± 0.7 (5) -
WT + Chol	40.9 ± 0.6 (5) ***	41.1 ± 2.0 (5) ns	46.4 ± 0.9 (5) ***
3xTg-AD	33.3 ± 1.2 (5) ns	38.7 ± 1.0 (5) ns	34.6 ± 0.6 (5) ns
3xTg-AD + Chol	34.8 ± 1.1 (5) §§§	33.0 ± 2.0 (5) § #	0/10 survived

Cholesterol diet causes significant weight gain in wildtype (WT) but not in triple-transgenic Alzheimer's disease (3xTg-AD) mice at 7 months.WT (129/C57BL6) and 3xTg-AD (B6;129-*Psen1*^{tm1Mpm}Tg(APPSwe, tauB301L)1Lfa/J) mice were fed a 5% cholesterol diet (Chol) from age 2 months and onwards. Animalweights were taken following behavioral testing and immediately prior to anesthesia and organ collection. Values represent mean weight in grams ± SEM. The number in parentheses provides the number of animals tested. Statistical analysis was performed using a one-way ANOVA and Fisher's LSD posthoc test. Symbols indicate the significant difference between groups compared toWT(*$p < 0.05$, ***$p < 0.001$, ns not significant), WT + cholesterol (§$p < 0.05$, §§§ $p < 0.001$) or 3xTg-AD (#$p < 0.05$).

Europe PMC Funders Author Manuscripts

Table 3

Effects of cholesterol diet on plasma corticosterone levels.

Group	7 months	14 months	20 months
WT	5905 ± 1080 (5) -	4810 ± 986 (5) -	4026 ± 1869 (5) -
WT + Chol	5748 ± 935 (5) ns	1795 ± 867 (5) *	3933 ± 1608 (5) ns
3xTg-AD	6145 ± 520 (5) ns	4226 ± 1061 (5) ns	7185 ± 804 (5) ns
3xTg-AD + Chol	4833 ± 1493 (5) ns	7195 ± 778 (5) §§§ #	0/10 survived

Plasma was collected following behavioral testing and immediately prior to anesthesia and organ collection. Values representmean plasma corticosterone in pg/ml ± SEM. The number in parentheses indicates the number of animals tested in each group. Statistical analysis was performed using a one-way ANOVA with a Fisher's LSD posthoc test. Symbols indicate the significant difference between groups compared toWT (*$p < 0.05$, ns not significant),WT + cholesterol (Chol) (§§§ $p < 0.001$) or 3xTg-AD (#$p < 0.05$).

Europe PMC Funders Author Manuscripts

Table 4

Summary of outcomes or pathologies for investigated mouse models.

Pathology/outcome	Measure	APPSwDI	WT + CHOL	3xTg-AD	3xTg-AD + CHOL
Diet	Weight	NA	↑↑↑	=	(↓)
Cholesterol diet	Plasma cholesterol	NA	↑↑	↑	↑
Cognitive function	Maze	NA	↓	↓↓	(↑)
Stress	Corticosterone	NA	↓	=	↑
AD-like	Aβ, PHF-tau	Aβ ↑↑↑	-	Aβ ↑↑	Aβ ↑
				Tau ↑↑	Tau ↑
Neuroinflammation	GFAP, Iba1, C1q	↑↑↑	↑	↑↑	=
					C1q ↑
BBB disruption	Mo IgG, ApoE	↑↑↑	↑	(↑)	=
Vessel staining	Collagen IV, tTG-2	↓	↑↑	=	↑